Electronic Supplementary Information

Effects of calcium on the kinetics of a model disjunctive ligand exchange reaction: Implications for dynamic trace metal speciation.[1]

Laura T. Rea

Yi Xu

Nathan E. Boland[2]

Whitman College, Department of Chemistry, Walla Walla, WA 99362, United States of America

---

[1] Electronic supplementary information (ESI) available.

[2] Corresponding Author at: Whitman College, Hall of Science, 345 Boyer Avenue, Walla Walla, WA 99362 USA, Phone: +1 (509) 527-5906, Fax: +1 (509) 527-5904, Email: bolandne@whitman.edu (N. E. Boland)

Rate Law Derivations

Rate expressions for adjunctive, semijunctive, and disjunctive ligand exchange pathways were described previously.[1,2] The derivations below are modified from Boland and Stone (2017).[1]

Rate Law for Adjunctive Ligand Exchange Pathways

Multidentate ligand exchange proceeds by an overall reaction where one multidentate ligand, L is replaced by another, Y, in the inner-coordination sphere of a metal, M.

$$ML + Y \rightarrow MY + L \tag{1}$$

The adjunctive pathway was described in the *Introduction* of the main text:

$$ML + Y \underset{k_{MLY'}^{-Y}}{\overset{k_{ML}^{Y}}{\rightleftharpoons}} MLY' \tag{2}$$

$$MLY' \xrightarrow{k_{MLY'}^{-L}} MY + L \tag{3}$$

where the apostrophe (‘) indicates a partially coordinated multidentate ligand and the rate constants k_{ML}^{Y}, $k_{MLY'}^{-Y}$, and $k_{MLY'}^{-L}$ are rate constants for the corresponding reactions. It is assumed that equilibrium lies far to the right of Reaction (3) so that the reverse reaction is ignored. The reaction intermediate, MLY’, is not expected to be particularly stable so [MLY’] will reach steady state rapidly:

$$\frac{d\left[MLY'\right]}{dt} = 0 = k_{ML}^{Y}\left[ML\right]\left[Y\right] - k_{MLY'}^{-Y}\left[MLY'\right] - k_{MLY'}^{-L}\left[MLY'\right] \tag{4}$$

So that the steady state concentration, $[MLY']_{ss}$, is defined by:

$$\left[MLY'\right]_{ss} = \frac{k_{ML}^{Y}\left[ML\right]\left[Y\right]}{k_{MLY'}^{-Y} + k_{MLY'}^{-L}} \tag{5}$$

Production of MY is given by:

$$\frac{d\left[MY\right]}{dt}=k_{MLY'}^{-L}\left[MLY'\right] \tag{6}$$

Combining Equations (5) and (6) gives:

$$\text{Adjunctive Rate Law} = \frac{d\left[MY\right]}{dt}=\frac{k_{ML}^{Y}k_{MLY'}^{-L}\left[ML\right]\left[Y\right]}{k_{MLY'}^{-Y}+k_{MLY'}^{-L}} \tag{7}$$

As noted previously,[1] rate constants are not necessarily for elementary steps in the reaction but for distinct stages of the overall reaction pathway.

Rate Law for Semijunctive Ligand Exchange Pathways

The semijunctive pathway was described in the *Introduction* of the main text:

$$ML \underset{k_{ML'}}{\overset{k_{ML}^{'}}{\rightleftharpoons}} ML' \tag{8}$$

$$ML'+Y \underset{k_{ML'Y'}^{-Y}}{\overset{k_{ML'}^{Y}}{\rightleftharpoons}} ML'Y' \tag{9}$$

$$ML'Y' \xrightarrow{k_{ML'Y'}^{-L}} MY+L \tag{10}$$

were the rate constants $k_{ML}^{'}$, $k_{ML'}$, $k_{ML'}^{Y}$, $k_{ML'Y'}^{-Y}$ and $k_{ML'Y'}^{-L}$ are rate constants for the corresponding reactions. Assuming that intermediates, ML’ and ML’Y’, are not stable and reach steady state quickly, we can define steady state concentrations, $[ML']_{ss}$ and $[ML'Y']_{ss}$:

$$\frac{d\left[ML'\right]}{dt}=0=k_{ML}^{'}\left[ML\right]-k_{ML'}\left[ML'\right]-k_{ML'}^{Y}\left[ML'\right]\left[Y\right] \tag{11}$$

$$\left[ML'\right]_{ss} = \frac{k^{'}_{ML}\left[ML\right]}{k_{ML'} + k^{Y}_{ML'}\left[Y\right]} \tag{12}$$

and

$$\frac{d\left[ML'Y'\right]}{dt} = 0 = k^{Y}_{ML'}\left[ML'\right]\left[Y\right] - k^{-Y}_{ML'Y'}\left[ML'Y'\right] - k^{-L}_{ML'Y}\left[ML'Y'\right] \tag{13}$$

$$\left[ML'Y'\right]_{ss} = \frac{k^{Y}_{ML'}\left[ML'\right]\left[Y\right]}{k^{-Y}_{ML'Y'} + k^{-L}_{ML'Y'}} \tag{14}$$

Production of MY is given by:

$$\frac{d\left[MY\right]}{dt} = k^{-L}_{ML'Y'}\left[ML'Y'\right] \tag{15}$$

Combining Equations (12), (14), and (15) gives a general rate expression:

$$\text{Semijunctive Rate Law} = \frac{d\left[MY\right]}{dt} = \frac{k^{'}_{ML}k^{Y}_{ML'}k^{-L}_{ML'Y'}\left[ML\right]\left[Y\right]}{\left(k_{ML'} + k^{Y}_{ML'}\left[Y\right]\right)\left(k^{-Y}_{ML'Y'} + k^{-L}_{ML'Y'}\right)} \tag{16}$$

The validity of the steady state assumptions in Equations (12) and (14) have been addressed previously.[1]

Disjunctive Ligand Exchange Pathway

The disjunctive pathway was described in the *Introduction* of the main text:

$$ML \underset{k^{M}_{L}}{\overset{k_{ML}}{\rightleftharpoons}} M + L \tag{17}$$

$$M + Y \xrightarrow{k^{M}_{Y}} MY \tag{18}$$

where the rate constants k_{ML}, k_L^M, and k_Y^M are rate constants for the corresponding reactions. Equilibrium lies far to the right of Reaction (18) so the reverse reaction is ignored. In the presence of two multidentate ligands, free metal ion concentrations, [M], will reach steady state rapidly:

$$\frac{d\left[ML'\right]}{dt} = 0 = k_{ML}\left[ML\right] - k_L^M\left[M\right]\left[L\right] - k_Y^M\left[M\right]\left[Y\right] \tag{19}$$

$$\left[M\right]_{ss} = \frac{k_{ML}\left[ML\right]}{k_L^M\left[L\right] + k_Y^M\left[Y\right]} \tag{20}$$

Production of MY is given by:

$$\frac{d\left[MY\right]}{dt} = k_Y^M\left[M\right]\left[Y\right] \tag{21}$$

Combining Equations (20) and (21) gives:

$$\text{Disjunctive Rate Law} = \frac{d\left[MY\right]}{dt} = \frac{k_{ML}k_Y^M\left[ML\right]\left[Y\right]}{k_L^M\left[L\right] + k_Y^M\left[Y\right]} \tag{22}$$

The rate expressions given above are in their generic forms, where multidentate ligand protonation and possible acid-catalyzed pathways are ignored.

Initial Rate Experiments

Ligand exchange reactions were initiated by rapidly mixing two solutions that were pre-equilibrated for at least 24 hours: Solution A containing 100 µM nickel chloride and 105 to 500 µM NTA and Solution B containing 105 to 1000 µM CDTA. Both solutions were prepared with identical concentrations of calcium chloride (varied from 0 to 2 mM) and 5 mM pH buffer, and sufficient NaCl to raise the ionic strength to 10 (±1) mM. A series of non-complexing pH buffers were used: DEPP ($4.2 < p^aH < 5.2$ and $8.3 < p^aH < 9.3$), MES ($5.7 < p^aH < 6.7$), and MOPS ($6.6 < p^aH < 7.6$).[3]

Ligand exchange reaction progress was monitored over time by analyzing aliquots of mixed reaction solution using a Beckman Coulter P/ACE MDQ capillary electrophoresis instrument (Brea, CA, USA) (recently acquired by AB Sciex, Framingham, MA, USA) with a photodiode array UV detector (Beckman-Coulter; Brea, CA). For short reaction timescales (1-18 hours), aliquots were drawn from reaction solution stored in the temperature-controlled chamber within the CE. For longer reaction timescales (>18 hrs), the reaction solution was stored in an external temperature-controlled chamber and transferred to the CE as needed. Separations were performed in a 47.5 cm long silica capillary with a detection window etched at 40 cm and an inner diameter of 75.4 µm. The capillary was cut to the appropriate length using a scoring tool, and the detection window was etched using concentrated sulfuric acid at 70 °C to remove the polyimide coating from the capillary. The coating was also removed on the ends of the capillary using flame.

Before separation, the capillary was preconditioned by rinsing (30 psi applied pressure) the capillary for five minutes with 0.1 M NaOH, then with ultrapure water for three minutes, and then a ten minute rinse with background electrolyte (BGE) containing 20 mM pyrophosphate (pH 7.1) and 0.4 mM TTAB surfactant.

The separation procedure began with a short (30 second) rinse with fresh BGE to remove air bubbles, followed by sample injection (0.5 psi for 15 seconds). The ends of the capillary were then placed in BGE, and -28 kV were applied. Each separation lasted 6 minutes with a 0.17 min ramp to optimize resolution. Absorbance peaks were observed at 214 nm.

Initial rates of reaction were determined by monitoring the formation of NiCDTA over time. Integrated peak areas were normalized by dividing by electromigration times to correct for run-to-run differences in electroosmotic flow rates. NiCDTA peak areas were calibrated with a series of six standard solutions containing fixed $CDTA_T$, Ca_T, pH buffer and varying Ni_T. The first 20% of reaction was fit using the linear least squares method to determine the initial rate of reaction (**Figure 3, main text**). The complete collection of initial rates is provided in **Table S1**.

Table S1. Initial Rates of Ni(cdta)$^{2-}$ formation follow ligand exchange between NiNTA and CDTA at 25 °C.

Ni$_T$ (μM)	NTA$_T$ (μM)	CDTA$_T$ (μM)	Ca$_T$ (μM)	Buffer	pH	d[NiCDTA]/dt (M s^{-1})[a]	Data points in first 20%
50	52.5	200	500	MOPS	6.55	$1.8(\pm1) \times 10^{-10}$	20
50	52.5	200	500	MOPS	6.55	$1.7(\pm1) \times 10^{-10}$	11
50	52.5	200	500	MES	6.07	$4.5(\pm7) \times 10^{-10}$	6
50	52.5	200	500	MES	6.07	$4.6(\pm7) \times 10^{-10}$	6
50	52.5	200	500	DEPP	4.36	$1.6(\pm4) \times 10^{-9}$	4
50	52.5	200	500	DEPP	4.36	$1.8(\pm5) \times 10^{-9}$	4
50	52.5	200	500	MOPS	6.98	$1.6(\pm1) \times 10^{-10}$	21
50	52.5	200	500	MOPS	6.98	$1.5(\pm1) \times 10^{-10}$	20
50	52.5	200	500	MOPS	7.78	$3.8(\pm3) \times 10^{-11}$	21
50	52.5	200	500	MOPS	7.46	$5.7(\pm4) \times 10^{-11}$	21
50	52.5	200	500	MOPS	7.46	$5.7(\pm4) \times 10^{-11}$	21
50	52.5	200	500	MOPS	7.78	$3.7(\pm2) \times 10^{-11}$	8
50	52.5	200	500	MOPS	7.78	$4.1(\pm2) \times 10^{-11}$	9
50	52.5	200	500	DEPP	8.41	$8.9(\pm4) \times 10^{-12}$	17
50	52.5	200	500	DEPP	8.41	$1.02(\pm5) \times 10^{-11}$	17
50	52.5	200	500	MES	5.40	$7.3(\pm4) \times 10^{-10}$	10
50	52.5	200	500	MES	5.40	$7.1(\pm1) \times 10^{-10}$	11
50	52.5	200	500	MOPS	7.78	$2.1(\pm2) \times 10^{-11}$	11
50	52.5	200	500	MOPS	7.78	$2.2(\pm2) \times 10^{-11}$	8
50	52.5	200	500	DEPP	8.41	$1.03(\pm2) \times 10^{-11}$	21
50	52.5	200	500	DEPP	8.41	$7.8(\pm3) \times 10^{-12}$	20
50	75	200	500	MES	5.41	$6.8(\pm4) \times 10^{-10}$	8
50	75	200	500	MES	5.41	$6.3(\pm2) \times 10^{-10}$	11
50	125	200	500	MES	5.45	$6.3(\pm3) \times 10^{-10}$	11
50	125	200	500	MES	5.45	$5.9(\pm3) \times 10^{-10}$	12
50	52.5	400	500	MES	5.50	$8.0(\pm4) \times 10^{-10}$	12
50	52.5	400	500	MES	5.50	$7.2(\pm2) \times 10^{-10}$	11
50	52.5	100	500	MES	5.41	$6.4(\pm4) \times 10^{-10}$	5
50	52.5	100	500	MES	5.41	$7.4(\pm3) \times 10^{-10}$	8
50	52.5	100	500	MES	5.41	$6.7(\pm3) \times 10^{-10}$	11
50	75	200	500	MOPS	6.98	$3.2(\pm1) \times 10^{-11}$	16
50	75	200	500	MOPS	6.98	$3.1(\pm1) \times 10^{-11}$	18
50	125	200	500	MOPS	6.95	$1.3(\pm3) \times 10^{-11}$	18
50	125	200	500	MOPS	6.95	$1.2(\pm2) \times 10^{-11}$	21
50	75	200	500	MOPS	6.98	$3.8(\pm2) \times 10^{-11}$	21
50	75	200	500	MOPS	6.98	$4.1(\pm2) \times 10^{-11}$	21
50	250	200	500	MOPS	6.97	$5.6(\pm2) \times 10^{-12}$	18
50	250	200	500	MOPS	6.97	$5.9(\pm1) \times 10^{-12}$	21
50	52.5	100	500	MOPS	6.91	$1.20(\pm5) \times 10^{-10}$	20
50	52.5	100	500	MOPS	6.91	$1.10(\pm5) \times 10^{-10}$	19

Ni_T (μM)	NTA_T (μM)	$CDTA_T$ (μM)	Ca_T (μM)	Buffer	pH	d[NiCDTA]/dt (M s^{-1})[a]	Data points in first 20%
50	52.5	400	500	MOPS	6.96	2.5(±2) x 10^{-10}	8
50	52.5	400	500	MOPS	6.96	2.8(±1) x 10^{-10}	8
50	75	200	500	MOPS	7.67	1.06(±4) x 10^{-11}	21
50	75	200	500	MOPS	7.67	1.00(±4) x 10^{-11}	21
50	125	200	500	MOPS	7.64	3.5(±1) x 10^{-12}	18
50	125	200	500	MOPS	7.64	3.54(±6) x 10^{-12}	18
50	52.5	100	500	MOPS	7.66	1.18(±5) x 10^{-11}	19
50	52.5	100	500	MOPS	7.66	1.41(±5) x 10^{-11}	21
50	52.5	400	500	MOPS	7.72	6.1(±5) x 10^{-11}	10
50	52.5	400	500	MOPS	7.72	5.7(±4) x 10^{-11}	12
50	52.5	200	250	MES	5.45	6.2(±4) x 10^{-10}	10
50	52.5	200	250	MES	5.45	6.5(±4) x 10^{-10}	11
50	52.5	200	1000	MES	5.40	6.1(±6) x 10^{-10}	6
50	52.5	200	1000	MES	5.40	6.0(±6) x 10^{-10}	5
50	52.5	200	1000	MES	5.40	9.1(±9) x 10^{-10}	4
50	52.5	200	250	MOPS	7.05	2.3(±2) x 10^{-10}	11
50	52.5	200	250	MOPS	7.05	2.5(±1) x 10^{-10}	11
50	52.5	200	1000	MOPS	7.00	6.9(±7) x 10^{-11}	10
50	52.5	200	1000	MOPS	7.00	7.7(±8) x 10^{-11}	11
50	52.5	200	250	MOPS	7.73	3.9(±5) x 10^{-11}	24
50	52.5	200	250	MOPS	7.73	4.4(±4) x 10^{-11}	24
50	52.5	200	1000	MOPS	7.67	3.1(±4) x 10^{-11}	9
50	52.5	200	1000	MOPS	7.67	3.1(±3) x 10^{-11}	9
50	52.5	200	1000	MOPS	7.67	3.3(±3) x 10^{-11}	15
50	52.5	200	1000	MOPS	7.67	3.5(±3) x 10^{-11}	15
50	52.5	500	1000	MOPS	6.79	2.3(±2) x 10^{-10}	16
50	52.5	500	1000	MOPS	6.79	2.0(±2) x 10^{-10}	16
50	52.5	400	1000	MOPS	6.80	1.9(±1) x 10^{-10}	18
50	52.5	400	1000	MOPS	6.80	2.2(±1) x 10^{-10}	18
50	52.5	300	1000	MOPS	6.82	1.7(±1) x 10^{-10}	18
50	52.5	300	1000	MOPS	6.82	1.9(±1) x 10^{-10}	18
50	52.5	200	210	MOPS	7.06	3.2(±1) x 10^{-10}	13
50	52.5	200	210	MOPS	7.06	3.3(±1) x 10^{-10}	12
50	52.5	200	2000	MOPS	7.06	9(±1)x 10^{-11}	18
50	52.5	200	2000	MOPS	7.06	1.1(±1) x 10^{-10}	15
50	52.5	200	1000	MOPS	6.86	1.7(±2) x 10^{-10}	15
50	52.5	200	1000	MOPS	6.86	1.4(±2) x 10^{-10}	16
50	52.5	200	1000	MOPS	6.86	1.5(±2) x 10^{-10}	18
50	52.5	200	1000	MOPS	6.86	1.7(±2) x 10^{-10}	17
50	52.5	200	1000	MOPS	6.86	1.5(±2) x 10^{-10}	16
50	52.5	200	1000	MOPS	6.86	1.3(±2) x 10^{-10}	15

Ni_T (μM)	NTA_T (μM)	$CDTA_T$ (μM)	Ca_T (μM)	Buffer	pH	d[NiCDTA]/dt (M s^{-1})[a]	Data points in first 20%
50	52.5	100	1000	MOPS	7.06	1.2(±2) x 10^{-10}	10
50	52.5	100	1000	MOPS	7.06	1.1(±2) x 10^{-10}	8
50	52.5	52.5	1000	MOPS	6.86	3(±1) x 10^{-11}	22
50	52.5	52.5	1000	MOPS	6.86	5.1(±9) x 10^{-11}	11
50	52.5	50	0	MOPS	6.96	3.8(±1) x 10^{-10}	9
50	52.5	50	0	MOPS	6.96	3.32(±6) x 10^{-10}	10
50	52.5	100	0	MOPS	6.96	3.7(±2) x 10^{-10}	8
50	52.5	100	0	MOPS	6.96	4.0(±2) x 10^{-10}	8
50	52.5	200	0	MOPS	6.96	3.3(±2) x 10^{-10}	9
50	52.5	200	0	MOPS	6.96	3.2(±2) x 10^{-10}	7
50	52.5	200	0	MOPS	6.96	4.0(±3) x 10^{-10}	13
50	52.5	325	0	MOPS	6.96	3.4(±2) x 10^{-10}	9
50	52.5	325	0	MOPS	6.96	3.5(±3) x 10^{-10}	8
50	52.5	500	0	MOPS	6.96	3.3(±3) x 10^{-10}	10
50	52.5	500	0	MOPS	6.96	3.0(±3) x 10^{-10}	9
50	52.5	200	0	MOPS	6.96	4.0(±3) x 10^{-10}	13
50	250	200	0	MOPS	6.96	4.4(±4) x 10^{-10}	4
50	500	200	0	MOPS	6.96	4.3(±4) x 10^{-10}	4

[a] Standard error in parentheses reflects error in the slope of the initial rate lines as reported by the LINEST function in Microsoft Excel 2016.

Equilibrium Calculations

The computer program HYDRAQL[4] was used to calculate equilibrium concentrations of nickel, calcium and multidentate ligand species present in Solution A, Solution B and mixed reaction solutions before and after equilibrium is attained. For input into HYDRAQL, published equilibrium constants[5] were converted to log K values at 0.0 M ionic strength using the Davies Equation (**Table S2**).[6]

Table S2 Relevant equilibrium constants[5] at an ionic strength of 0.0 M[a] and 25°C

Equation	Log K	Equation	Log K
$H_4(nta)^+ = H_3(nta)^0 + H^+$	-0.9	$Ni^{2+} + nta^{3-} = Ni(nta)^-$	12.83
$H_3(nta)^0 = H_2(nta)^- + H^+$	-2.0	$Ni^{2+} + 2nta^{3-} = Ni(nta)_2{}^{4-}$	16.98
$H_2(nta)^- = H(nta)^{2-} + H^+$	-2.96	$Ni(OH)(nta)^{2-} + H^+ = Ni(nta)^-$	11.30
$H(nta)^{2-} = nta^{3-} + H^+$	-10.32	$Ca^{2+} + nta^{3-} = Ca(nta)^-$	7.6
		$Ca^{2+} + 2nta^{3-} = Ca(nta)_2{}^{4-}$	9.47
$H_5(cdta)^+ = H_4(cdta)^0 + H^+$	-1.6[b]		
$H_4(cdta)^0 = H_3(cdta)^- + H^+$	-2.70	$Ni^{2+} + cdta^{4-} = Ni(cdta)^{2-}$	22.0
$H_3(cdta)^- = H_2(cdta)^{2-} + H^+$	-3.9	$Ni(cdta)^{2-} + H^+ = NiH(cdta)^-$	2.74[b]
$H_2(cdta)^{2-} = H(cdta)^{3-} + H^+$	-6.73	$Ca^{2+} + cdta^{4-} = Ca(cdta)^{2-}$	14.9
$H(cdta)^{3-} = cdta^{4-} + H^+$	-13.2		
		$Ni(OH)_2(s, am) + 2\ H^+ = Ni^{2+} + 2H_2O$	12.7
$Ca(OH)_2(s,am) + 2H^+ = Ca^{2+} + 2H_2O$	5.3	$Ni^{2+} + H_2O = NiOH^+ + H^+$	-9.9
$Ca^{2+} + H_2O = CaOH^+ + H^+$	-12.7	$Ni^{2+} + 2H_2O = Ni(OH)_2 + 2H^+$	-19
		$Ni^{2+} + 3H_2O = Ni(OH)_3{}^- + 3H^+$	-30
		$4\ Ni^{2+} + 4\ H_2O = Ni_4(OH)_4{}^{4+} + 4\ H^+$	-27.7

[a] Where necessary, log K values were corrected to I = 0.0 M with activity coefficients calculated using the Davies Equation, $\log \gamma_{\pm z} = -0.5\, z^2 \left(\frac{\sqrt{I}}{1+\sqrt{I}} - 0.2\, I\right)$, unless otherwise noted.

[b] log K at I = 1.0 M. Due to the limitations of the Davies Equation this value was not converted to I = 0.0 M.

Including Calcium in Rate Calculations

Ligand exchange between NiNTA and CDTA proceeds via a disjunctive pathway (see main text):

$$Ni(nta)^{-} \underset{k_{L}^{Ni}}{\overset{k_{NiL}}{\rightleftharpoons}} Ni^{2+} + nta^{3-} \tag{23}$$

$$Ni(nta)^{-} + H^{+} \underset{k_{HL}^{Ni}}{\overset{k_{NiL}^{H}}{\rightleftharpoons}} Ni^{2+} + H(nta)^{2-} \tag{24}$$

$$Ni^{2+} + cdta^{4-} \xrightarrow{k_{Y}^{Ni}} Ni(cdta)^{2-} \tag{25}$$

$$Ni^{2+} + H(cdta)^{3-} \xrightarrow{k_{HY}^{Ni}} Ni(cdta)^{2-} + H^{+} \tag{26}$$

where the rate constants k_{NiL}, k_{L}^{Ni}, k_{NiL}^{H}, k_{HL}^{Ni}, k_{Y}^{Ni} and k_{HY}^{Ni} are rate constants for the corresponding reactions. In the presence of calcium, the pathway remains disjunctive, but additional reactions between calcium and free multidentate ligand must be considered when calculating reaction rates:

$$Ca^{2+} + nta^{3-} \underset{k_{CaL}}{\overset{k_{L}^{Ca}}{\rightleftharpoons}} Ca\left(nta\right)^{-} \tag{27}$$

$$Ca^{2+} + H(nta)^{3-} \underset{k_{Cal}^{H}}{\overset{k_{HL}^{Ca}}{\rightleftharpoons}} Ca\left(nta\right)^{-} + H^{+} \tag{28}$$

$$Ca^{2+} + cdta^{4-} \underset{k_{CaY}}{\overset{k_{Y}^{Ca}}{\rightleftharpoons}} Ca\left(cdta\right)^{2-} \tag{29}$$

$$Ca^{2+} + H\left(cdta\right)^{3-} \underset{k_{CaY}^{H}}{\overset{k_{HY}^{Ca}}{\rightleftharpoons}} Ca\left(cdta\right)^{2-} + H^{+} \tag{30}$$

where the rate constants k_{CaL}, k_{L}^{Ca}, k_{CaL}^{H}, k_{HL}^{Ca}, k_{Y}^{Ca}, k_{CaY}, k_{HY}^{Ca}, and k_{CaY}^{H} are rate constants for the corresponding reactions. Rate constants for the Reactions (23) through (30) are available (**Table S3**).

Note that complex formation and dissociation rate constants for calcium, k_Y^{Ca} and k_{HY}^{Ca} are much greater than for nickel complexes, k_Y^{Ni} and k_{HY}^{Ni}, respectively. Furthermore, in all our experiments, Ca_T is in excess of NTA_T and $CDTA_T$ combined and Ni_T is less than either NTA_T or $CDTA_T$, so free calcium will be in large excess of free nickel. Therefore, it is a reasonable assumption that calcium, free multidentate ligands, and calcium-multidentate ligand complexes reach a pre-equilibrium state prior to significant formation of significant concentrations of $Ni(cdta)^{2-}$.

Table S3. Rate constants for relevant reactions

Reaction	**Rate Constant**	**Value**[a]	**Source (Conditions)**
$Ni(nta)^- \rightarrow Ni^{2+} + nta^{3-}$	k_{NiL}	$7.0\ (\pm 0.4) \times 10^{-6}\ s^{-1}$	[1](I = 0.01 M)
		$5.8 \times 10^{-6}\ s^{-1}$	[7](I = 0.4M)
		$3.5 \times 10^{-6}\ s^{-1}$	[7](I = 1.25 M)
$Ni^{2+} + nta^{3-} \rightarrow Ni(nta)^-$	k_L^{Ni}	$4.8 \times 10^5\ M^{-1}s^{-1}$	[7](I = 1.25 M)
		$3.5\ (\pm 0.2) \times 10^6\ M^{-1}s^{-1}$	This work (I = 0.01 M)
$H^+ + Ni(nta)^- \rightarrow Ni^{2+} + H(nta)^{2-}$	k_{NiL}^H	$1.93\ (\pm 0.08)\ M^{-1}s^{-1}$	[1](I = 0.01 M)
		0.77	[7](I = 0.4M)
		0.43	[7](I = 1.25 M)
$Ni^{2+} + H(nta)^{2-} \rightarrow H^+ + Ni(nta)^-$	k_{HL}^{Ni}	$7.5\ M^{-1}s^{-1}$	[7](I = 1.25 M)
		$9\ M^{-1}s^{-1}$	This work (I = 0.01 M)
$Ni^{2+} + H_2(cdta)^{2-} \rightarrow Ni(cdta)^{2-} + 2H^+$	k_{H2Y}^{Ni}	$8.0 \times 10^3\ M^{-1}s^{-1}$	[8](I = 0.3 M)
$Ni^{2+} + H(cdta)^{3-} \rightarrow Ni(cdta)^{2-} + H^+$	k_{HY}^{Ni}	$3.6(\pm 0.3) \times 10^5\ M^{-1}s^{-1}$	[9](I = 0.1 M)
		$1.9 \times 10^5\ M^{-1}s^{-1}$	[8](I = 0.3 M)
$Ni^{2+} + edta^{4-} \rightarrow Ni(edta)^{2-}$	k_Y^{Ni}	$6 \times 10^6\ M^{-1}s^{-1}$	[10](I = 0.01 M)
$Ca^{2+} + cdta^{4-} \rightarrow Ca(cdta)^{2-}$	k_Y^{Ca}	1.4×10^9	[11](I = 0.5 M)
$Ca(cdta)^{2-} \rightarrow Ca^{2+} + cdta^{4-}$	k_{CaY}	$3.0(\pm 0.1) \times 10^{-5}\ s^{-1}$	[11](I = 0.5 M)
$Ca^{2+} + H(cdta)^{3-} \rightarrow Ca(cdta)^{2-} + H^+$	k_{HY}^{Ca}	1.7×10^6	[11](I = 0.5 M)
$Ca(cdta)^{2-} + H^+ \rightarrow Ca^{2+} + H(cdta)^{3-}$	k_{CaY}^H	$7.1 \times 10^5\ M^{-1}s^{-1}$	[9](I = 0.1 M)
		$4.4(\pm 0.1) \times 10^5\ M^{-1}s^{-1}$	[11](I = 0.5 M)

[a] Reported uncertainty is the standard error in the least squares fit of all rate data to the kinetic model.

Derivation of Overall Rate Law for Ni(cdta)$^{2-}$ Formation

The following is the derivation of the rate law for formation of Ni(cdta)$^{2-}$ by the disjunctive ligand exchange between NiNTA and CDTA.

The formation of Ni(cdta)$^{2-}$ is occurs by reactions (25) and (26) yielding the rate equation

$$\frac{d\left[Ni\left(cdta\right)^{2-}\right]}{dt}=\left(k_{Y}^{Ni}\left[cdta^{4-}\right]+k_{HY}^{Ni}\left[H\left(cdta\right)^{3-}\right]\right)\left[Ni^{2+}\right] \tag{31}$$

The concentration of free Ni^{2+} is the result of formation via reactions (23) and (24), and consumption via reactions (25) and (26) and the reverse of reactions (23) and (24). Given the competition between various multidentate ligands, the [Ni^{2+}] will rapidly reach a steady state

$$\frac{d\left[Ni^{2+}\right]}{dt}=0=\left(k_{NiL}+k_{NiL}^{H}\left[H^{+}\right]\right)\left[Ni\left(nta\right)^{-}\right]-\left(k_{L}^{Ni}\left[nta^{3-}\right]+k_{HL}^{Ni}\left[H\left(nta\right)^{2-}\right]\right)\left[Ni^{2+}\right]-\left(k_{Y}^{Ni}\left[cdta^{4-}\right]+k_{HY}^{Ni}\left[H\left(cdta\right)^{3-}\right]\right)\left[Ni^{2+}\right]$$

(32)

The steady state concentration for free Ni^{2+}, [Ni^{2+}]$_{SS}$, is found by rearranging equation (32).

$$\left[Ni^{2+}\right]_{SS}=\frac{\left(k_{NiL}+k_{NiL}^{H}\left[H^{+}\right]\right)\left[Ni\left(nta\right)^{-}\right]}{\left(k_{L}^{Ni}\left[nta^{3-}\right]+k_{HL}^{Ni}\left[H\left(nta\right)^{2-}\right]\right)+\left(k_{Y}^{Ni}\left[cdta^{4-}\right]+k_{HY}^{Ni}\left[H\left(cdta\right)^{3-}\right]\right)} \tag{33}$$

We note that formation of Ni^{2+} by reactions (23) and (24) can be thought of as un-catalyzed and acid-catalyzed pathways. We can distinguish between these two pathways by separating the summation in the numerator of equation (33)

$$\left[Ni^{2+}\right]_{SS,0}=\frac{k_{NiL}\left[Ni\left(nta\right)^{-}\right]}{\left(k_{L}^{Ni}\left[nta^{3-}\right]+k_{HL}^{Ni}\left[H\left(nta\right)^{2-}\right]\right)+\left(k_{Y}^{Ni}\left[cdta^{4-}\right]+k_{HY}^{Ni}\left[H\left(cdta\right)^{3-}\right]\right)} \tag{34}$$

$$\left[Ni^{2+}\right]_{ss,H} = \frac{k_{NiL}^{H}\left[H^{+}\right]\left[Ni\left(nta\right)^{-}\right]}{\left(k_{L}^{Ni}\left[nta^{3-}\right]+k_{HL}^{Ni}\left[H\left(nta\right)^{2-}\right]\right)+\left(k_{Y}^{Ni}\left[cdta^{4-}\right]+k_{HY}^{Ni}\left[H\left(cdta\right)^{3-}\right]\right)} \qquad (35)$$

Substituting equations (34) and (35) into equation (31) gives the rate of formation of $Ni(cdta)^{2-}$ via an uncatalyzed pathway (R_0) and an acid-catalyzed pathway (R_H), respectively.

$$R_0 = \frac{d\left[Ni(cdta)^{2-}\right]}{dt} = \frac{k_{NiL}\left[Ni(nta)^{-}\right]\left(k_{Y}^{Ni}\left[cdta^{4-}\right]+k_{HY}^{Ni}\left[H(cdta)^{3-}\right]\right)}{\left(k_{L}^{Ni}\left[nta^{3-}\right]+k_{HL}^{Ni}\left[H(nta)^{2-}\right]\right)+\left(k_{Y}^{Ni}\left[cdta^{4-}\right]+k_{HY}^{Ni}\left[H(cdta)^{3-}\right]\right)}$$

(36)

$$R_H = \frac{d\left[Ni(cdta)^{2-}\right]}{dt} = \frac{k_{NiL}^{H}\left[H^{+}\right]\left[Ni(nta)^{-}\right]\left(k_{Y}^{Ni}\left[cdta^{4-}\right]+k_{HY}^{Ni}\left[H(cdta)^{3-}\right]\right)}{\left(k_{L}^{Ni}\left[nta^{3-}\right]+k_{HL}^{Ni}\left[H(nta)^{2-}\right]\right)+\left(k_{Y}^{Ni}\left[cdta^{4-}\right]+k_{HY}^{Ni}\left[H(cdta)^{3-}\right]\right)}$$

(37)

The overall rate of $Ni(cdta)^{2-}$ formation, R_T, is given by the sum of equations (36) and (37)

$$\frac{d\left[Ni(cdta)^{2-}\right]}{dt} = R_T = R_0 + R_H = \frac{\left(k_{NiL}+k_{NiL}^{H}\left[H^{+}\right]\right)\left[Ni(nta)^{-}\right]\left(k_{Y}^{Ni}\left[cdta^{4-}\right]+k_{HY}^{Ni}\left[H(cdta)^{3-}\right]\right)}{\left(k_{L}^{Ni}\left[nta^{3-}\right]+k_{HL}^{Ni}\left[H(nta)^{2-}\right]\right)+\left(k_{Y}^{Ni}\left[cdta^{4-}\right]+k_{HY}^{Ni}\left[H(cdta)^{3-}\right]\right)}$$

(38)

To extend the rate law to all disjunctive ligand exchange reactions, a more generic rate law can be written:

$$\frac{d\left[MY\right]}{dt} = R_T = R_0 + R_H = \frac{\left(k_{ML}+k_{MiL}^{H}\left[H^{+}\right]\right)\left[ML\right]\sum_{n} k_{H_nY}^{M}\left[H_nY\right]}{\sum_{n} k_{H_nL}^{M}\left[H_nL\right]+\sum_{n} k_{H_nY}^{M}\left[H_nY\right]} \qquad (39)$$

where H_nL and H_nY are the *n* protonation levels of L and Y, respectively.

Alternative Kinetic Model Fitting

The rate law in equation (38) was fit to the initial rates in **Table S1**. Input initial concentrations were calculated as described in the main text *Equilibrium and Rate Modeling*. Given the availability of rate constants (**Table S3**) and equilibrium constants (**Table 1, main text,** corrected for ionic strength 0.01 M) for the relevant reactions, there are multiple ways to select rate constant values for calculating initial rates using equation (38). Before enumerating the different ways to select constants, here are the principles by which we judged each approach:

A. The most appropriate constants are obtained under similar experimental conditions (e.g. temperature, pH, ionic strength).
B. Model optimization should be used to determine the values for constants that are least certain.
C. The model should be optimized by varying the fewest possible number of fitting parameters.
D. The goodness of fit is quantified by the sum of the square differences between calculated and experimental initial rates, $\sum d^2$.

Model optimization was achieved by minimizing squared differences between log initial rates from kinetic experiments (**Table S1**) and those calculated by equation (38). The standard errors in fitted values, as well as standard error in the minimized sum of squared differences, were obtained using SolverAid, a macro for determining non-linear least squares statistics published with the Macrobundle for Excel software package.[12]

Table S4. Evaluation of Model Fitting Options

Option 1 (*preferred)*	Option 2	Option 3	Option 4	Option 5
fit *k_L^{Ni}, k_{HL}^{Ni}*	***fit*** *k_L^{Ni}, k_{HL}^{Ni}, k_{HY}^{Ni}*	*calculated k_L^{Ni}, k_{HL}^{Ni} from K_{NiL} and k_{NiL}, and K_{NiL}^H and k_{NiL}^H*	***fit*** *k_L^{Ni}, k_{HL}^{Ni}, k_{NiL}, k_{NiL}^H, but constrain by K_{NiL} and K_{NiL}^H*	***fit*** *k_L^{Ni}, k_{HL}^{Ni}, k_{NiL}, k_{NiL}^H, but constrain by K_{NiL} and K_{NiL}^H* ***fit*** *k_{HY}^{Ni}*
Inputs: k_{NiL} = 7.0(±0.4)x10^{-6} s^{-1} **k_L^{Ni} = 3.5(±0.2)x10^6 M^{-1}s^{-1}** k_{NiL}^H = 1.93(±0.08) M^{-1}s^{-1} **k_{HL}^{Ni} = 9* M^{-1}s^{-1}** k_{HY}^{Ni} = 3.6(±0.3)x10^5 M^{-1}s^{-1} k_Y^{Ni} = 6x10^6 M^{-1}s^{-1} *uncertain	***Inputs:*** k_{NiL} = 7.0(±0.4)x10^{-6} s^{-1} **k_L^{Ni} = 1x10^7* M^{-1}s^{-1}** k_{NiL}^H = 1.93(±0.08) M^{-1}s^{-1} **k_{HL}^{Ni} = 24* M^{-1}s^{-1}** k_{HY}^{Ni} = 3.6(±0.3)x10^5 M^{-1}s^{-1} **k_Y^{Ni} = 1x10^6* M^{-1}s^{-1}** *uncertain	***Inputs:*** k_{NiL} = 7.0(±0.4)x10^{-6} s^{-1} k_L^{Ni} = 1.39(±0.08)x10^7 M^{-1}s^{-1} k_{NiL}^H = 1.93(±0.08) M^{-1}s^{-1} k_{HL}^{Ni} = 342(±14) M^{-1}s^{-1} k_{HY}^{Ni} = 3.6(±0.3)x10^5 M^{-1}s^{-1} k_Y^{Ni} = 6x10^6 M^{-1}s^{-1}	***Inputs:*** **k_{NiL} = 9.7(±0.1)x10^{-6} s^{-1}** **k_L^{Ni} = 1.94(±0.03)x10^7 M^{-1}s^{-1}** **k_{NiL}^H = 0.9(±0.1) M^{-1}s^{-1}** **k_{HL}^{Ni} = 170(±20) M^{-1}s^{-1}** k_{HY}^{Ni} = 3.6(±0.3)x10^5 M^{-1}s^{-1} k_Y^{Ni} = 6x10^6 M^{-1}s^{-1}	***Inputs:*** **k_{NiL} = 6.44(±0.03)x10^{-6} s^{-1}** **k_L^{Ni} = 1.28(±0.01)x10^7 M^{-1}s^{-1}** **k_{NiL}^H = 1.45(±0.05) M^{-1}s^{-1}** **k_{HL}^{Ni} = 257(±8) M^{-1}s^{-1}** **k_{HY}^{Ni} = 1.49(±0.09)x10^6 M^{-1}s^{-1}** k_Y^{Ni} = 6x10^6 M^{-1}s^{-1}
$\sum d^2$ = 2.29 (±0.15)	$\sum d^2$ = 2.29 (±0.15)	$\sum d^2$ = 18.3 (±0.4)	$\sum d^2$ = 17.9(±0.4)	$\sum d^2$ = 2.14 (±0.14)
Evaluation Criteria: A. True B. True C. 2 parameters D. 2nd (tie)	***Evaluation Criteria:*** A. True B. True C. 3 parameters D. 2nd (tie)	***Evaluation Criteria:*** A. False B. False C. 0 parameters D. 6th	***Evaluation Criteria:*** A. False B. Partially True C. 2 parameters D. 5th	***Evaluation Criteria:*** A. False B. Partially True C. 3 parameters D. 1st
Overall: **Good**	***Overall:*** **Poor**	***Overall:*** **Poor**	***Overall:*** **Poor**	***Overall:*** **Fair**

Table S4 – Continued.
Option 6 ***fit*** *k_L^{Ni},* ***fit*** *k_{HL}^{Ni}, k_{NiL}^H, but constrained by K_{NiL}^H*
Inputs: k_{NiL} = 7.0(±0.4)x10^{-6} s^{-1} **k_L^{Ni} = 3.3 (±0.2)x10^6 M^{-1}s^{-1}** **k_{NiL}^H = 1.31(±0.04) M^{-1}s^{-1}** **k_{HL}^{Ni} = 231(±8) M^{-1}s^{-1}** k_{HY}^{Ni} = 3.6(±0.3)x10^5 M^{-1}s^{-1} k_Y^{Ni} = 6x10^6 M^{-1}s^{-1} $\sum d^2$ = 2.26 (±0.15) ***Evaluation Criteria Rank:*** A. Partially True B. Partially True C. 2 parameters D. 2nd (tie) ***Overall:*** **Fair**

We evaluated six options for how to fit the model to experimental data based on the criteria above (**Table S4**):

Option 1: Use published values for k_{NiL}, k_{NiL}^{H}, k_{HY}^{Ni}, and k_{Y}^{Ni} and use least squares fitting to optimize k_{L}^{Ni} and k_{HL}^{Ni}. Previously reported values for k_L^{Ni} and k_{HL}^{Ni} are the least certain of potential model inputs: they were obtained at very high ionic strength (1.25 M) and were reported without uncertainties. Least squares fitting yielded values that are within an order of magnitude of the previously reported values (**Table S3**). Unfortunately, the standard error for the fitted value of k_{HL}^{Ni} was greater than the value itself, so it should be considered provisional. Only two parameters were optimized to yield a model fit with relatively low $\sum d^2$. It is noted, however, k_{HL}^{Ni}/k_{NiL}^{H} equals $10^{0.68}$, which is a bit low compared to the expected equilibrium constant for $Ni(nta)^{1-}$ formation (the reverse of reaction (24)), $K_{ML}^{H} = 10^{2.25}$, calculated from values in **Table 1**. Plots of this model fit to experimental data are shown in **Figure S1**.

Option 2: Use published values for k_{NiL}, k_{NiL}^{H}, and k_{Y}^{Ni} and use least squares fitting to optimize k_{L}^{Ni}, k_{HL}^{Ni}, k_{HY}^{Ni}. This option is similar to the first option, but adds least squares fitting to obtain a value of k_{HY}^{Ni}, which is the only other rate constant in Eqn. (38) for which we do not have a value at 0.01 M ionic strength. Unfortunately, k_{HY}^{Ni} has a high level of collinearity with k_L^{Ni} and k_{HL}^{Ni} (as determined by SolverAid).[12] As a result, fitting all three rate constants yielded uncertainties of each that are greater than the values themselves. So, despite a similarly good fit to our experimental data as Option 1, the model result is of less value. Plots of this model fit to experimental data are shown in **Figure S2**.

Option 3: Use published values for k_{NiL}, k_{NiL}^{H}, k_{HY}^{Ni}, and k_{Y}^{Ni} and use equilibrium constants to calculate k_{L}^{Ni} and k_{HL}^{Ni}. No least squares fitting parameters are required in this option. Note that the ratio of k_L^{Ni}/k_{NiL} yields the equilibrium constant, K_{NiL}, for $Ni(nta)^{1-}$ formation from nta^{3-} (the reverse of reaction (23)) and the ratio of k_{HL}^{Ni}/k_{NiL}^{H} yields the equilibrium constant, K_{NiL}^{H}, for $Ni(nta)^{1-}$ formation from $H(nta)^{2-}$ (the reverse of reaction (24). If we start with the ionic strength corrected equilibrium constants K_{NiL} ($10^{11.70}$)

and K_{NiL}^{H} ($10^{2.25}$) and the published values of k_{NiL} and k_{NiL}^{H} (**Table S3**) we calculate k_{L}^{Ni} = 1.39 (±0.08) x 10^7 $M^{-1}s^{-1}$ and k_{HL}^{Ni} = 342(±14) $M^{-1}s^{-1}$, respectively. Using these values, however, yields a very poor fit to the data, which is clear from the $\sum d^2$ value and the plots of the model fit to experimental data (**Figure S3**). We note that we have used constants from multiple sources and that we used the semi-empirical Davies equation to adjust the equilibrium constants from an ionic strength of 0.1 M to 0.01 M. We also note that the calculated value of k_{L}^{Ni} is at least an order of magnitude higher than rate constants for similar reactions between Ni^{2+} and other multidentate ligands with a +3 charge.[13] Similarly, the calculated value of k_{HL}^{Ni} is over an order of magnitude higher than previously reported rate constants for the same reaction (**Table S3**). Based on these observations, we suspect that the ionic strength corrected values of K_{NiL} and K_{NiL}^{H} (**Table 1**) are about an order of magnitude too high.

Option 4: Use published values for k_{HY}^{Ni}, and k_{Y}^{Ni}. Use least squares fitting to optimize values of k_{L}^{Ni}, k_{NiL}, k_{HL}^{Ni}, and k_{NiL}^{H}, but constrain values with the associated equilibrium constants. The formation rate constants (k_{L}^{Ni} and k_{HL}^{Ni}) and dissociation rate constants (k_{HL}^{Ni} and k_{NiL}^{H}) can be constrained by the formation equilibrium constants (K_{NiL} and K_{NiL}^{H}). If we assume microscopic irreversibility for the formation and dissociation reactions, then it is true that

$$k_f / k_d = K_f \tag{40}$$

where, k_f is the formation rate constant, k_d is the dissociation rate constant, and K_f is the associated formation equilibrium constant. Accordingly, we also note the following two equations are true

$$\log k_f - \log k_d = \log K_f \tag{41}$$

$$\log k_f + \log k_d = \log C \tag{42}$$

where C is a constant. The rate constants k_f and k_d can be determined from K_f and C

$$k_f = 10^{\frac{\left(\log K_f + \log C\right)}{2}} \tag{43}$$

$$k_f = 10^{\frac{\left(\log K_f - \log C\right)}{2}} \tag{44}$$

Using this method, we obtained the values for k_L^{Ni}, k_{HL}^{Ni}, k_{NiL}, and k_{NiL}^{H} reported in **Table S4**. We note that, again, the value of k_L^{Ni} is at least an order of magnitude higher than rate constants for similar reactions. Furthermore, the model fit to experimental data is relatively poor (**Figure S4**).

Option 5: Use the published value for k_Y^{Ni}. Use least squares fitting to optimize the value of k_{HY}^{Ni}. Use least squares fitting to optimize values of k_L^{Ni}, k_{NiL}, k_{HL}^{Ni}, and k_{NiL}^{H}, but constrain them with equilibrium constants. This modeling option follows the same approach as Option 4 for determining the values of k_L^{Ni}, k_{HL}^{Ni}, k_d, and k_{NiL}^{H}, but uses least squares fitting to optimize the value of k_{HY}^{Ni}. This option has the most fitting parameters (three) so it is not surprising that it yields the lowest $\sum d^2$ of the six options, albeit only slightly lower than Options 1 and 2. The value of k_{HY}^{Ni} is a bit higher than expected as compared to previously reported values and like Options 3 and 4, the value of k_L^{Ni} is high. Plots of this model fit to experimental data are shown in **Figure S5**.

Option 6: Use published values for k_{NiL}, k_L^{Ni}, k_{HY}^{Ni}, and k_Y^{Ni}. Use least squares fitting to optimize the value of k_L^{Ni}. Use least squares fitting to optimize values of k_{HL}^{Ni} and k_{NiL}^{H}, but constrain them with the equilibrium constant, K_{NiL}^{H}. Option 6 is a compromise between Options 1 and 5. Direct optimization of k_L^{Ni} yields a lower and more reasonable than is found by Option 5, while constraining k_{HL}^{Ni} and k_{NiL}^{H} by the value of K_{NiL}^{H} ensures corrects the ratio of k_{HL}^{Ni}/k_{NiL}^{H} is not too low as it was in Option 1. Only two parameters are optimized and yields a fit that is slightly better than Option 1, and slightly worse than Option 5. However, the modeling approach is inconsistent and, therefore, more contrived than in the other options. Plots of this model fit to experimental data are shown in **Figure S6**.

Considering all six options for model fitting in light of criteria A through D, we selected Option 1 as the preferred model fit. Option 1 uses literature values for rates constants that were collected under similar conditions and optimizes only two remaining values. It also produces a model fit that closely follows the experimental data. And while in terms of $\sum d^2$, it is slightly out performed by Options 5 and 6, the later options are not as successful in fitting rates at low pH and in the absence of Ca and have their own drawbacks as described above.

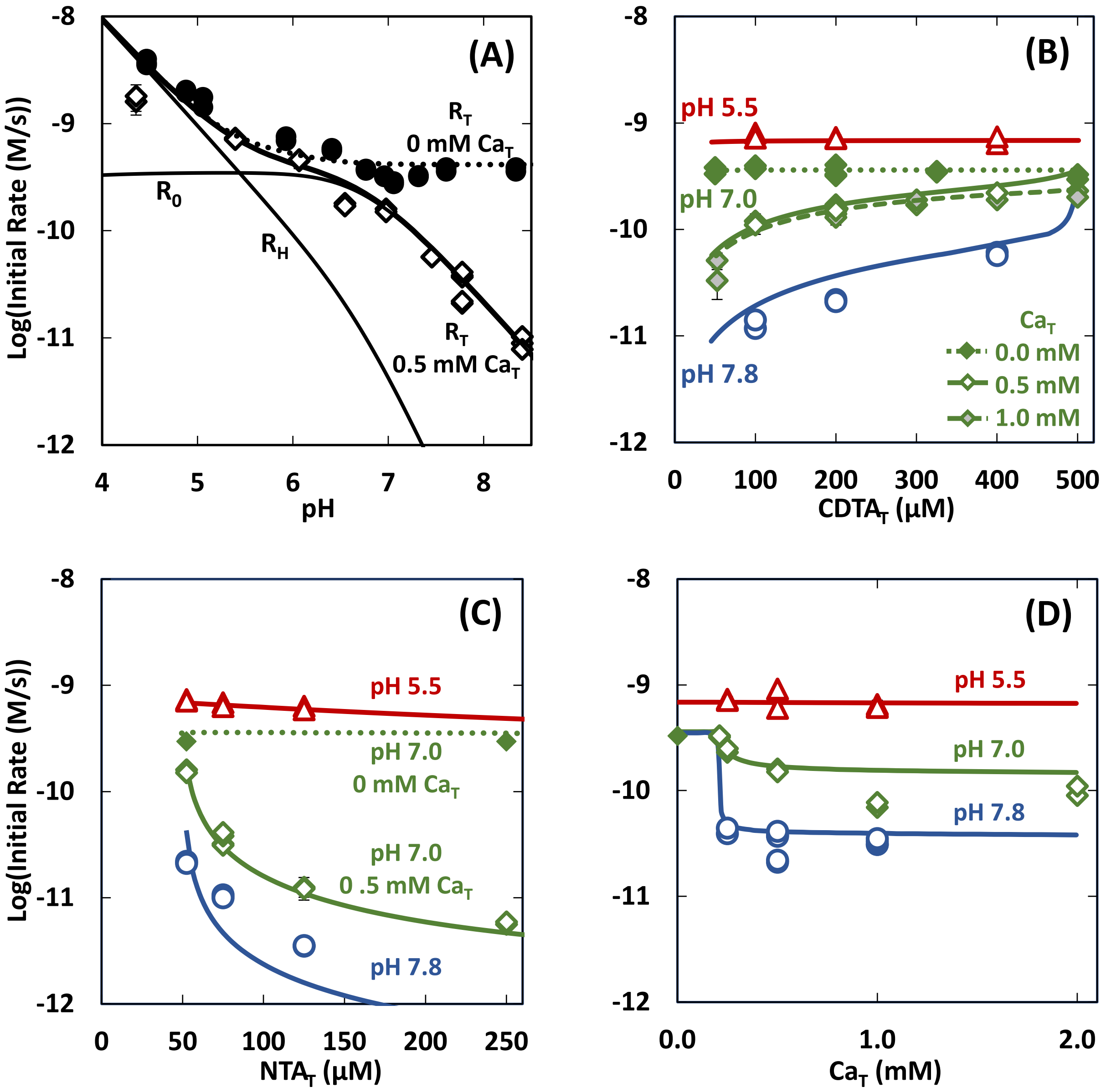

Figure S1. Option 1 model fit to initial rates of ligand exchange as a function of reaction conditions: (A) pH, (B) $CDTA_T$, (C) NTA_T, (D) Ca_T. Reaction conditions: 50 μM Ni_T, 5.0 mM pH buffer, and sufficient NaCl to fix the ionic strength at 10 mM; in (A): 200 μM $CDTA_T$, 52.5 μM NTA_T, 0.0 mM Ca_T (solid symbols)[28] or 0.5 mM Ca_T (open symbols); in (B): 52.5 μM NTA_T, and 0.0 mM Ca_T (solid symbols),[28] 0.5 mM Ca_T (open symbols) or 1.0 mM Ca_T (shaded symbols); in (C): 200 μM $CDTA_T$, and 0.0 mM Ca_T (solid symbols)[28] or 0.5 mM Ca_T (open symbols); and in (D): 200 μM $CDTA_T$, 52.5 μM NTA_T. Lines indicate modeled rates.

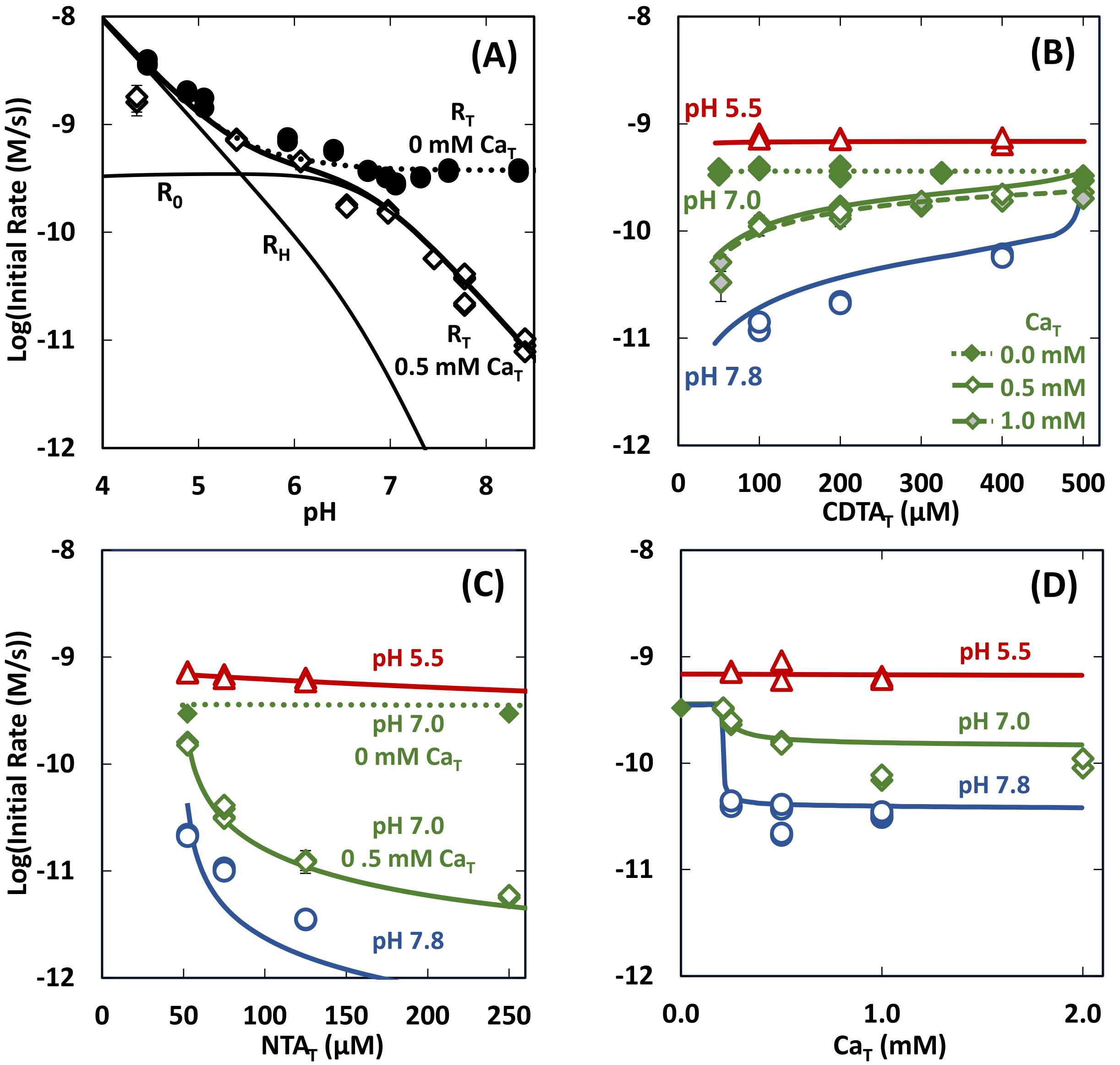

Figure S2. Option 2 model fit to initial rates of ligand exchange as a function of reaction conditions: (A) pH, (B) $\mathrm{CDTA_T}$, (C) $\mathrm{NTA_T}$, (D) $\mathrm{Ca_T}$. Reaction conditions: 50 µM $\mathrm{Ni_T}$, 5.0 mM pH buffer, and sufficient NaCl to fix the ionic strength at 10 mM; in (A): 200 µM $\mathrm{CDTA_T}$, 52.5 µM $\mathrm{NTA_T}$, 0.0 mM $\mathrm{Ca_T}$ (solid symbols)[28] or 0.5 mM $\mathrm{Ca_T}$ (open symbols); in (B): 52.5 µM $\mathrm{NTA_T}$, and 0.0 mM $\mathrm{Ca_T}$ (solid symbols),[28] 0.5 mM $\mathrm{Ca_T}$ (open symbols) or 1.0 mM $\mathrm{Ca_T}$ (shaded symbols); in (C): 200 µM $\mathrm{CDTA_T}$, and 0.0 mM $\mathrm{Ca_T}$ (solid symbols)[28] or 0.5 mM $\mathrm{Ca_T}$ (open symbols); and in (D): 200 µM $\mathrm{CDTA_T}$, 52.5 µM $\mathrm{NTA_T}$. Lines indicate modeled rates.

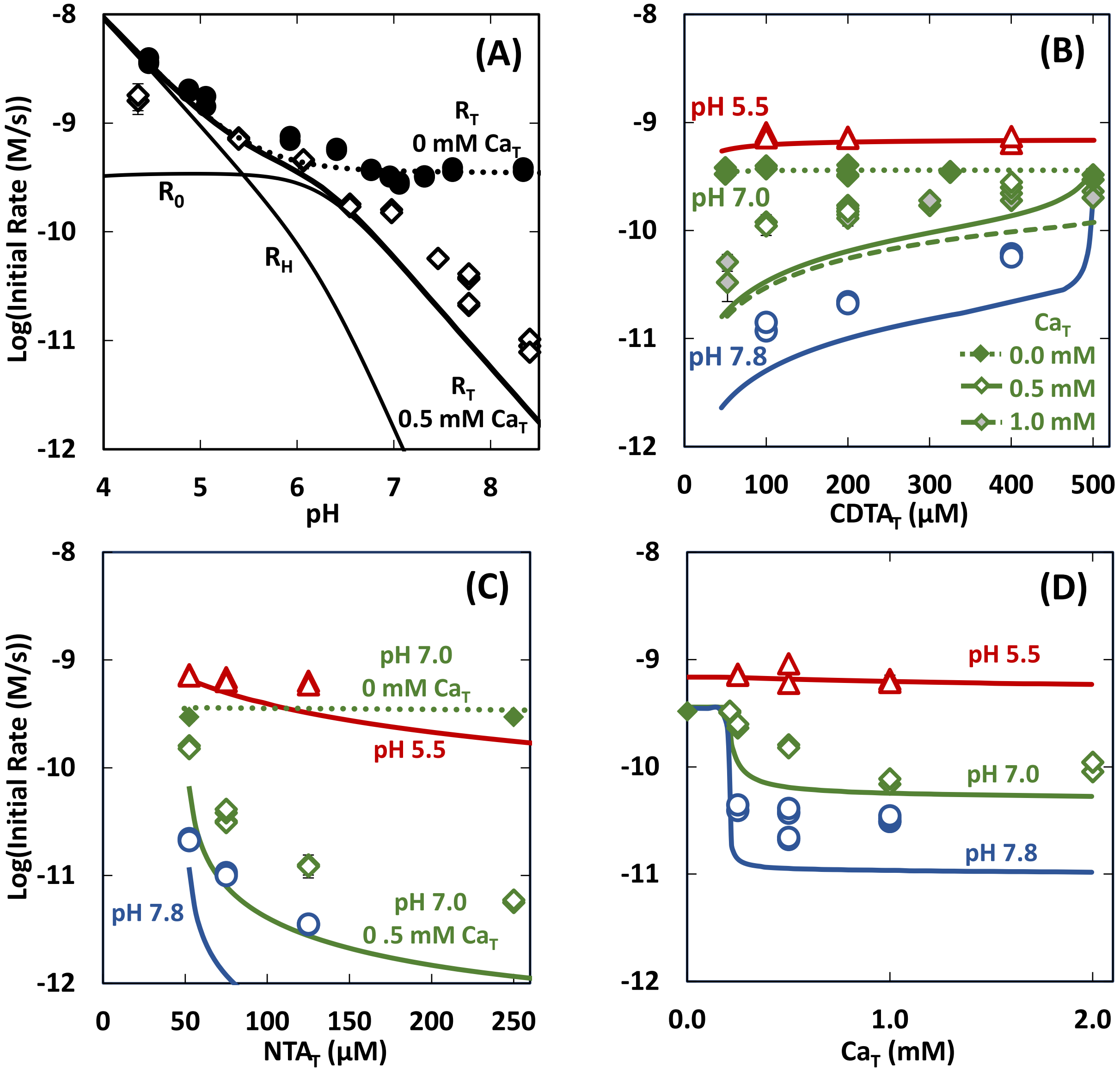

Figure S3. Option 3 model fit to initial rates of ligand exchange as a function of reaction conditions: (A) pH, (B) $CDTA_T$, (C) NTA_T, (D) Ca_T. Reaction conditions: 50 μM Ni_T, 5.0 mM pH buffer, and sufficient NaCl to fix the ionic strength at 10 mM; in (A): 200 μM $CDTA_T$, 52.5 μM NTA_T, 0.0 mM Ca_T (solid symbols)[28] or 0.5 mM Ca_T (open symbols); in (B): 52.5 μM NTA_T, and 0.0 mM Ca_T (solid symbols),[28] 0.5 mM Ca_T (open symbols) or 1.0 mM Ca_T (shaded symbols); in (C): 200 μM $CDTA_T$, and 0.0 mM Ca_T (solid symbols)[28] or 0.5 mM Ca_T (open symbols); and in (D): 200 μM $CDTA_T$, 52.5 μM NTA_T. Lines indicate modeled rates.

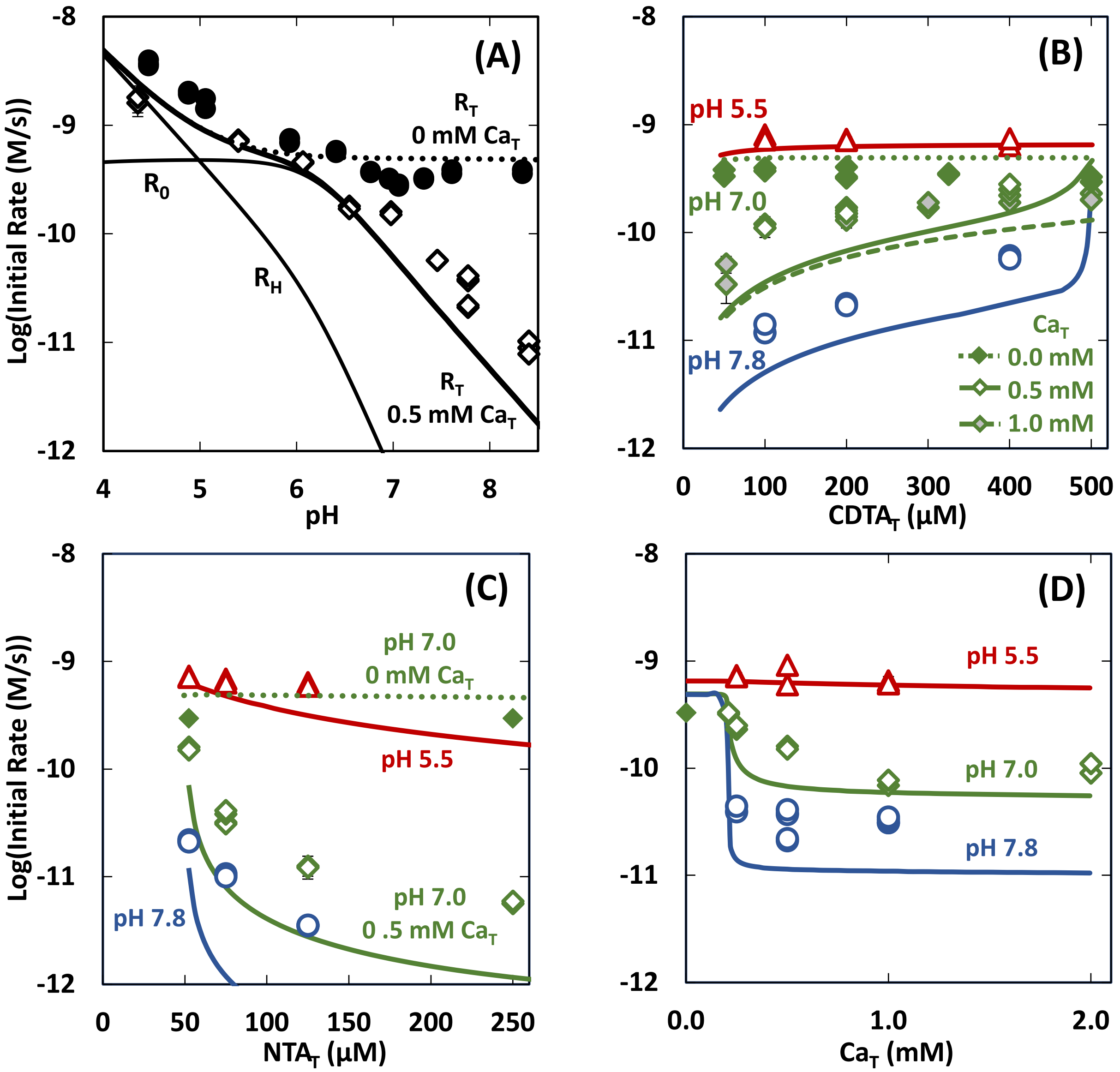

Figure S4. Option 4 model fit to initial rates of ligand exchange as a function of reaction conditions: (A) pH, (B) CDTA$_T$, (C) NTA$_T$, (D) Ca$_T$. Reaction conditions: 50 µM Ni$_T$, 5.0 mM pH buffer, and sufficient NaCl to fix the ionic strength at 10 mM; in (A): 200 µM CDTA$_T$, 52.5 µM NTA$_T$, 0.0 mM Ca$_T$ (solid symbols)[28] or 0.5 mM Ca$_T$ (open symbols); in (B): 52.5 µM NTA$_T$, and 0.0 mM Ca$_T$ (solid symbols),[28] 0.5 mM Ca$_T$ (open symbols) or 1.0 mM Ca$_T$ (shaded symbols); in (C): 200 µM CDTA$_T$, and 0.0 mM Ca$_T$ (solid symbols)[28] or 0.5 mM Ca$_T$ (open symbols); and in (D): 200 µM CDTA$_T$, 52.5 µM NTA$_T$. Lines indicate modeled rates.

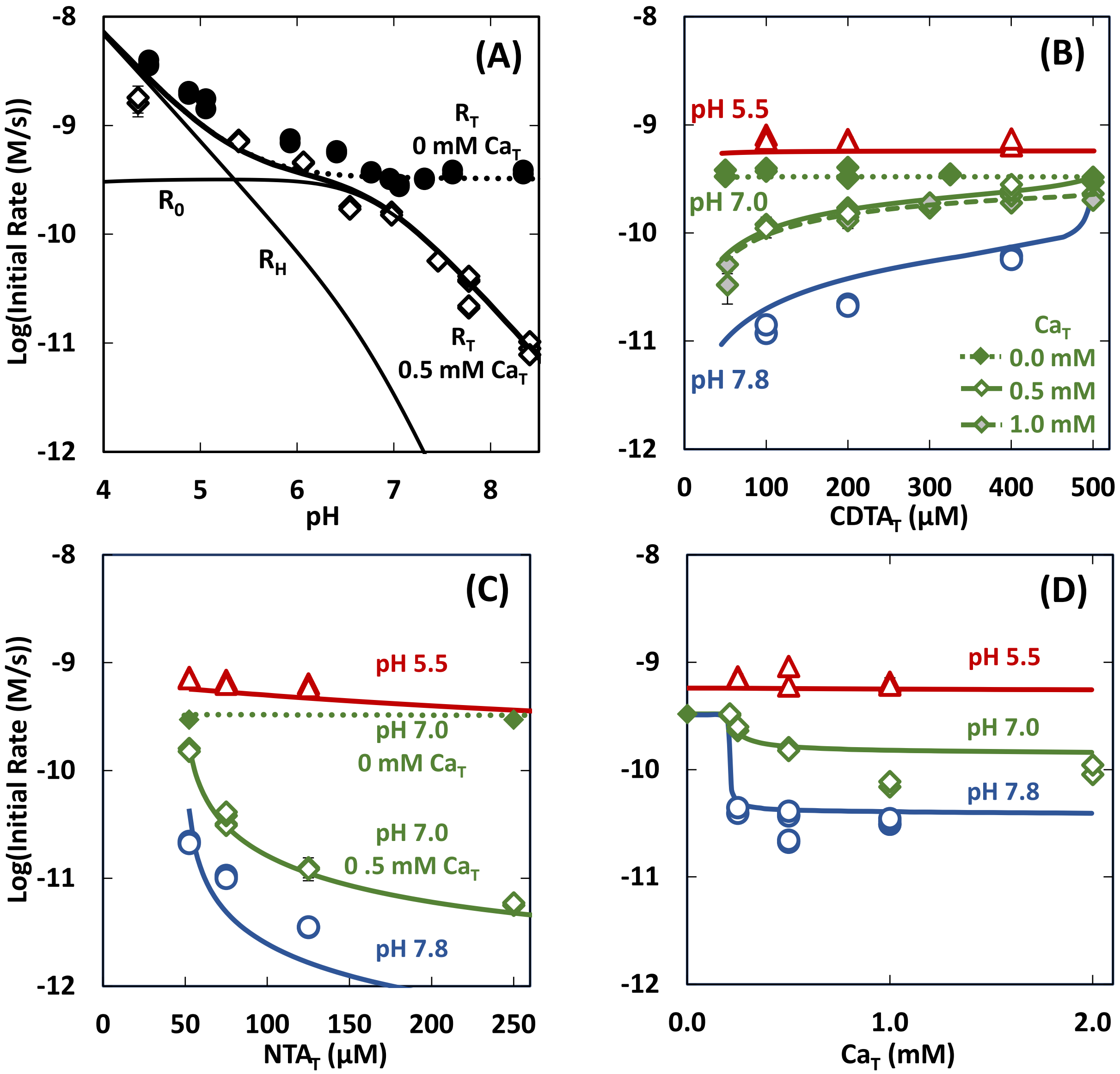

Figure S5. Option 5 model fit to initial rates of ligand exchange as a function of reaction conditions: (A) pH, (B) CDTA$_T$, (C) NTA$_T$, (D) Ca$_T$. Reaction conditions: 50 µM Ni$_T$, 5.0 mM pH buffer, and sufficient NaCl to fix the ionic strength at 10 mM; in (A): 200 µM CDTA$_T$, 52.5 µM NTA$_T$, 0.0 mM Ca$_T$ (solid symbols)[28] or 0.5 mM Ca$_T$ (open symbols); in (B): 52.5 µM NTA$_T$, and 0.0 mM Ca$_T$ (solid symbols),[28] 0.5 mM Ca$_T$ (open symbols) or 1.0 mM Ca$_T$ (shaded symbols); in (C): 200 µM CDTA$_T$, and 0.0 mM Ca$_T$ (solid symbols)[28] or 0.5 mM Ca$_T$ (open symbols); and in (D): 200 µM CDTA$_T$, 52.5 µM NTA$_T$. Lines indicate modeled rates.

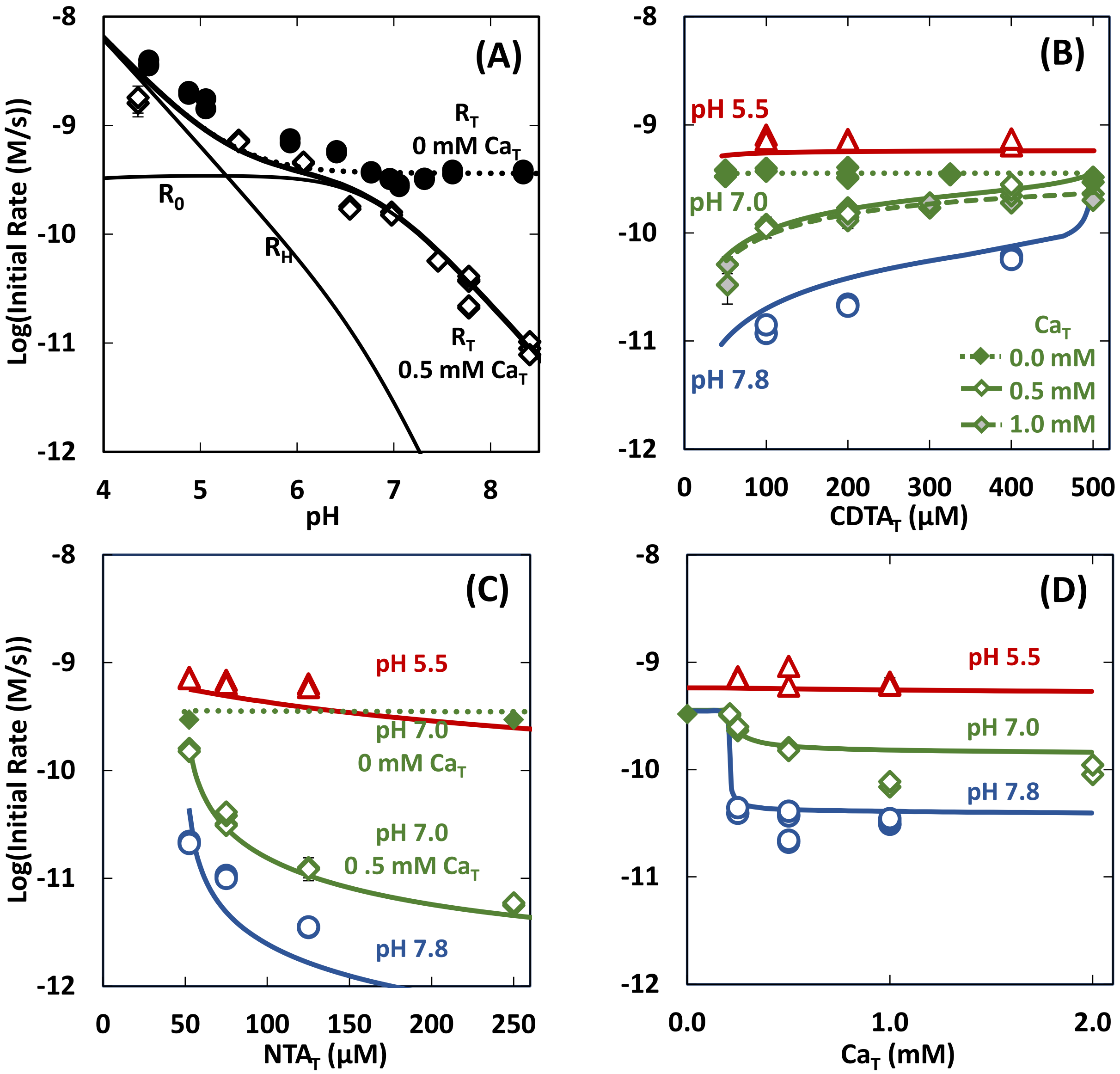

Figure S6. Option 6 model fit to initial rates of ligand exchange as a function of reaction conditions: (A) pH, (B) CDTA$_T$, (C) NTA$_T$, (D) Ca$_T$. Reaction conditions: 50 µM Ni$_T$, 5.0 mM pH buffer, and sufficient NaCl to fix the ionic strength at 10 mM; in (A): 200 µM CDTA$_T$, 52.5 µM NTA$_T$, 0.0 mM Ca$_T$ (solid symbols)[28] or 0.5 mM Ca$_T$ (open symbols); in (B): 52.5 µM NTA$_T$, and 0.0 mM Ca$_T$ (solid symbols),[28] 0.5 mM Ca$_T$ (open symbols) or 1.0 mM Ca$_T$ (shaded symbols); in (C): 200 µM CDTA$_T$, and 0.0 mM Ca$_T$ (solid symbols)[28] or 0.5 mM Ca$_T$ (open symbols); and in (D): 200 µM CDTA$_T$, 52.5 µM NTA$_T$. Lines indicate modeled rates.

References

1 N. E. Boland and A. T. Stone, Rates of nickel(II) capture from complexes with NTA, EDDA, and related tetradentate chelating agents by the hexadentate chelating agents EDTA and CDTA: Evidence of a 'semijunctive' ligand exchange pathway, Geochim. Cosmochim. Acta, 2017, 212, 176–195.

2 J. G. Hering and F. M. M. Morel, Kinetics of trace metal complexation: ligand-exchange reactions, Environ. Sci. Technol., 1990, 24, 242–252.

3 Q. Yu, A. Kandegedara, Y. Xu and D. B. Rorabacher, Avoiding interferences from Good's buffers: A contiguous series of noncomplexing tertiary amine buffers covering the entire range of pH 3-11, Anal. Biochem., 1997, 253, 50–56.

4 C. Papelis, K. F. Hayes and J. O. Leckie, HYDRAQL. Technical Report 306, Stanford, CA, 1988.

5 A. E. Martell, R. M. Smith and R. J. Motekaitis, NIST Critically Selected Stability Constants of Metal Complexes Database, version 8.0, National Institute of Science and Technology, Gaithersburg, MD, USA, 2004.

6 W. Stumm and J. J. Morgan, Aquatic Chemistry: Chemical Equilibria and Rates in Natural Waters, John Wiley & Sons, Inc., New York, NY, 3rd edn., 1996.

7 T. J. Bydalek and M. L. Blomster, Kinetics of the substitution reaction between copper(II) and nitrilotracetatonickelate(II), Inorg. Chem., 1964, 3, 667–671.

8 J. C. Cassatt and R. G. Wilkins, Kinetics of reaction of nickel(II) ion with a variety of amino acids and pyridinecarboxylates, J. Am. Chem. Soc., 1968, 90, 6045–6050.

9 D. W. Margerum, P. J. Menardi and D. L. Janes, Multidentate ligand kinetics. X. Exchange reactions of metal(II)-cyclohexylenediaminetetraacetate complexes, Inorg. Chem., 1967, 6, 283–289.

10 G. A. Rechnitz and Z. Lin, Reaction rate measurements with cation-sensitive glass electrodes. Kinetic study of the exchange reaction between silver(I)-EDTA and nickel(II), Anal. Chem., 1967, 39, 1406–1411.

11 J. D. Carr and D. G. Swartzfager, Kinetics of the ligand exchange and dissociation reactions of calcium-aminocarboxylate complexes, J. Am. Chem. Soc., 1975, 97, 315–321.

12 R. de Levie, MacroBundle for Excel, version 12, Brunswick, ME, USA, 2012.

13 D. W. Margerum, G. R. Cayley, D. C. Weatherburn and G. K. Pagenkopf, in Coordination Chemistry, ed. A. E. Martell, American Chemical Society, Washington, DC, 1978, vol. 2, pp. 1–220.